

Presented at the 2005 Spring Meeting of the European Materials Research Society, Strasbourg, 31.5.-3.6.2005

## LATTICE SITES OF IMPLANTED Cu AND Ag IN ZnO

U. Wahl,<sup>\*1,2</sup> E. Rita,<sup>1,2</sup> J.G. Correia,<sup>1,2,3</sup> T. Agne,<sup>3,4</sup> E. Alves,<sup>1,2</sup> J.C. Soares,<sup>2</sup> and the ISOLDE collaboration<sup>3</sup><sup>1</sup> Instituto Tecnológico e Nuclear, Estrada Nacional 10, 2686-953 Sacavém, Portugal<sup>2</sup> Centro de Física Nuclear da Universidade de Lisboa, 1649-003 Lisboa, Portugal<sup>3</sup> CERN-PH, 1211 Genève 23, Switzerland<sup>4</sup> Technische Physik, Universität des Saarlandes, 66123 Saarbrücken, Germany

### Abstract

The group Ib impurities Cu and Ag on substitutional Zn sites are among possible candidates for p-type doping of ZnO. In order to explore possible lattice sites of Cu and Ag in ZnO the radioactive impurities <sup>67</sup>Cu and <sup>111</sup>Ag were implanted at doses of  $4 \times 10^{12} \text{ cm}^{-2}$  to  $1 \times 10^{14} \text{ cm}^{-2}$  at 60 keV into ZnO single crystals. The emission channeling effects of  $\beta^-$  particles from the decay were studied by means of position-sensitive electron detectors, giving direct evidence that in the as-implanted state large fractions of Cu and Ag atoms (60-70% for Cu and 30% for Ag) occupy almost ideal substitutional Zn sites with root mean square (rms) displacements of 0.014-0.017 nm. However, following vacuum annealing at 600°C and above both Cu and Ag were found to be located increasingly on sites that are characterized by large rms displacements (0.03-0.05 nm) from Zn sites. We conclude that in high-temperature treated ZnO Cu and Ag are most likely not simply replacing Zn atoms but are incorporated in complexes with other crystal defects or as clusters.

**Keywords:** ZnO, Cu, Ag, ion implantation, emission channeling, lattice location

### Introduction

Finding a suitable acceptor impurity for reliable p-type doping remains one of the questions that urgently need to be solved in order to allow the realization of ZnO-based devices. Besides elements of group V of the periodic system replacing for O, also the group Ib impurities Cu and Ag on substitutional Zn sites have been considered as possible candidates for p-type doping [1]. Cu has been reported as a common impurity in ZnO crystals, and concentrations up to the ppm range are given in the literature [2-5]. Early resistivity measurements showed a decrease in n-type conductivity in Cu-doped ZnO, indicating the acceptor character of Cu. However, the decrease in n-type conductivity was found to be proportional to the square of the Cu concentration, which was explained by the passivation of Cu<sub>Zn</sub> acceptors by O vacancies [6,7] or the formation of acceptor-type Cu<sup>2+</sup>-Cu<sup>2+</sup> pairs [8]. More recently, admittance spectroscopy experiments found only deep acceptor levels located 0.17 eV below the conduction band for Cu [9] and 0.23 eV below the conduction band for Ag [10]. For Ag, which was also investigated with respect to its application in ZnO varistors, it was suggested that it acts as an amphoteric dopant, existing both on substitutional Zn sites and in the interstitial form [11]. Both for Cu and Ag it is hence questionable whether these Ib elements are actually incorporated on ideal substitutional Zn sites.

The role of Cu is also interesting due to its possible relation with the so-called "structured" green luminescence band frequently found in ZnO. While many authors [2-5, 12] have attributed the green luminescence to the Cu impurity, its role has also been questioned and native defects such as Zn vacancies [13,14], O antisite defects [15] or O vacancies [16-18] are being considered as possible candidates, too. Recent photoluminescence experiments using radioactive isotopes of Cu and Ni have given strong evidence that the structured green luminescence is actually caused by Zn vacancies [19].

We have previously studied the lattice location of implanted Cu [20] and Ag [21] in ZnO by means of the  $\beta^-$  emission channeling effect [22] from radioactive <sup>67</sup>Cu and <sup>111</sup>Ag isotopes. Our experimental method is based on the fact that the  $\beta^-$  particles that are emitted during nuclear decay experience channeling or blocking effects along major crystallographic axes and planes. The resulting anisotropic emission yield from the crystal surface characterizes the lattice site occupied by the probe atoms. In this paper we present additional data on <sup>67</sup>Cu-implanted samples with different doses and compare the behaviour of both group Ib impurities.

### Method

60 keV implantation of <sup>67</sup>Cu ( $t_{1/2} = 61.9 \text{ h}$ ) and <sup>111</sup>Ag ( $t_{1/2} = 7.45 \text{ d}$ ) was done by means of CERN's on-line isotope separator facility ISOLDE, which provides clean beams of these radioactive isotopes. The samples were all c-axis oriented, commercially available single-crystals, and purchased either from Eagle Picher Technologies and grown by the seeded chemical vapour transport (SCVT) process, or from Crystec GmbH and grown by the hydrothermal (HT) method. Five samples with the following characteristics were investigated: sample 1 HT-grown, O face, implanted dose  $4 \times 10^{12} \text{ cm}^{-2}$  of <sup>67</sup>Cu; sample 2 SCVT-grown, Zn face,  $2.3 \times 10^{13} \text{ cm}^{-2}$  of <sup>67</sup>Cu; sample 3 HT-grown, O face,  $1 \times 10^{14} \text{ cm}^{-2}$  of <sup>67</sup>Cu; sample 4 SCVT-grown, Zn face,  $2 \times 10^{13} \text{ cm}^{-2}$  of <sup>67</sup>Cu; sample 5 SCVT-grown, Zn face,  $2.0 \times 10^{13} \text{ cm}^{-2}$  of <sup>111</sup>Ag.

\* Corresponding author: Tel +351-219946085; Fax +351-219941525; Email: uwahl@itn.pt.

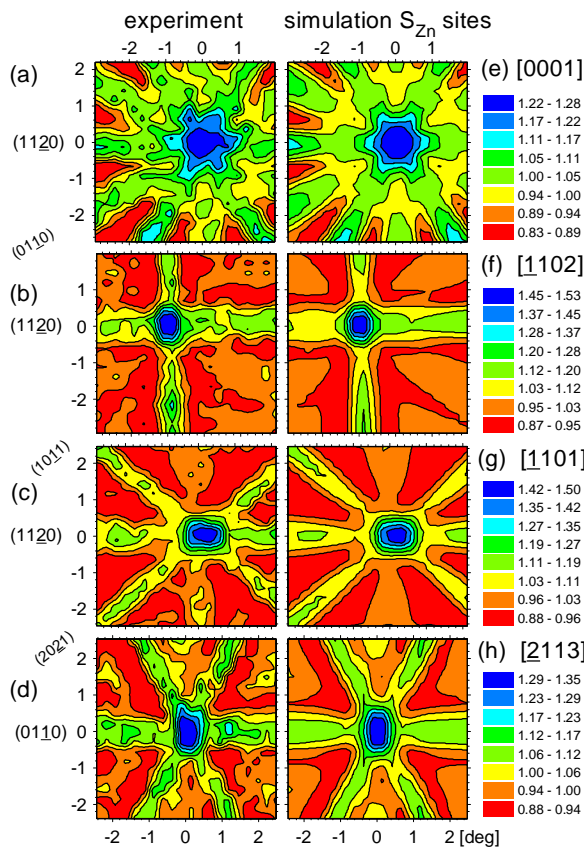


**Fig. 1:** Normalized angular-dependent  $\beta^-$  emission yields from  $^{67}\text{Cu}$  in ZnO sample 3, in the as-implanted state, around the crystalline axes (a) [0001], (b) [1102], (c) [1101] and (d) [2113]. Panels (f)-(h) represent the best two-fraction fit of theoretical patterns to the experimental data, corresponding to 62%, 52%, 55%, and 51% of Cu atoms on substitutional Zn sites  $S_{\text{Zn}}$ , with rms displacements perpendicular to the corresponding axes of  $u_1 = 0.017$  nm, 0.016 nm, 0.015 nm, and 0.014 nm, respectively.

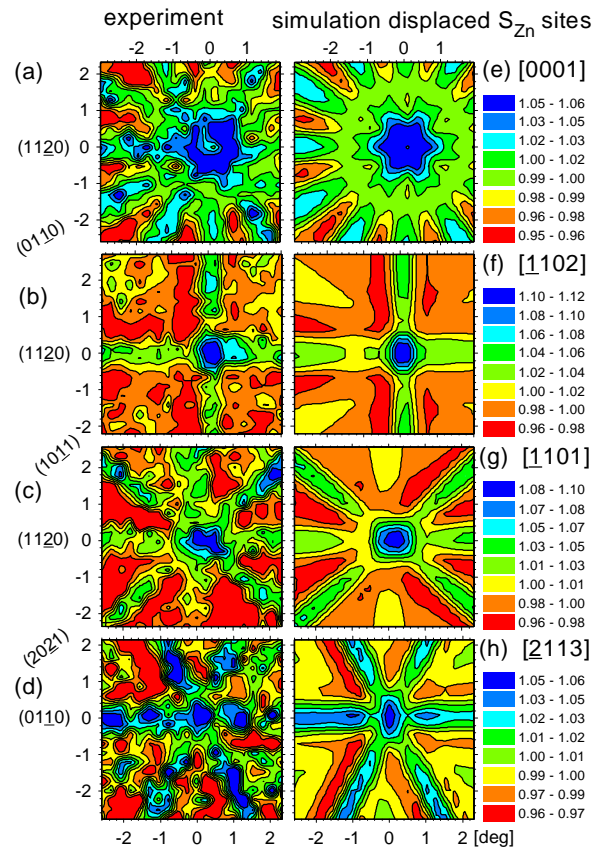


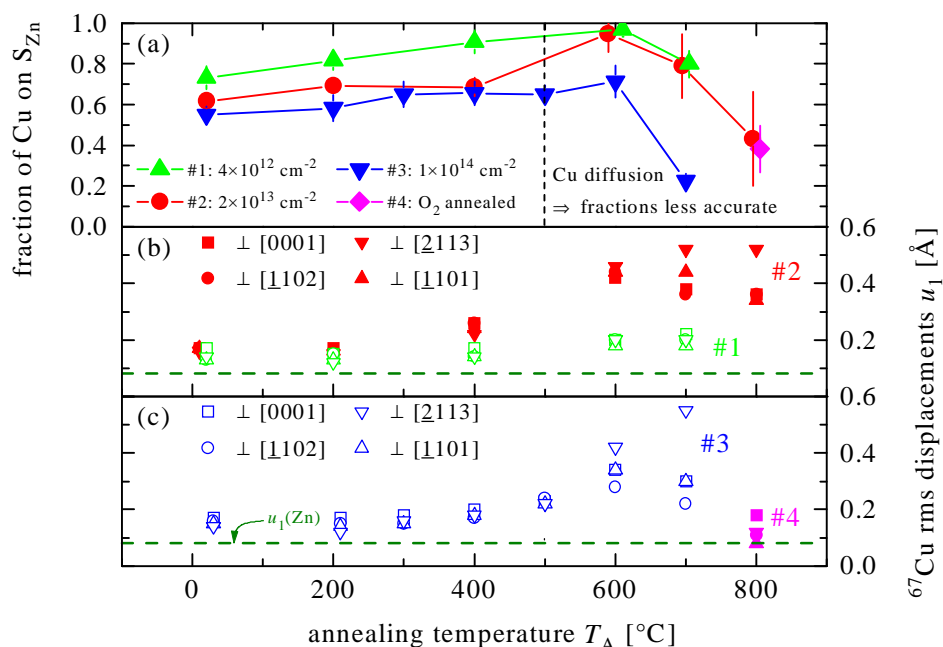
**Fig. 2:** Emission channeling patterns from  $^{67}\text{Cu}$  in ZnO sample 3, annealed at  $700^\circ\text{C}$  around the crystalline axes (a) [0001], (b) [1102], (c) [1101] and (d) [2113]. Panels (f)-(h) represent the best two-fraction fit of theoretical patterns to the experimental data, corresponding to 24%, 17%, and 23% of Cu atoms on displaced substitutional Zn sites, with rms displacements perpendicular to the corresponding axes of  $u_1 = 0.030$  nm, 0.022 nm, 0.030 nm, and 0.055 nm, respectively.

Lattice location experiments were carried out for samples 1-3 and 5 in the as-implanted state and after 10-min annealing sequences in vacuum up to  $700^\circ\text{C}$  or  $800^\circ\text{C}$ , while sample 4 was only investigated following annealing for 10 min under  $\text{O}_2$  atmosphere at  $800^\circ\text{C}$  in a sealed quartz crucible. The angle-dependent electron emission yield was measured by means of position-sensitive Si detectors [23]. The quantitative assignment of probe atom lattice sites was accomplished by fitting the experimental emission yields around [0001], [1102], [1101], and [2113] directions by theoretical channeling patterns for different lattice sites. We tried substitutional Zn and substitutional O sites, the main interstitial sites in the wurtzite structure such as T, O, H, BC and AB [24], and a variety of interstitial sites that are obtained by displacing the probe atoms along bonding or anti-bonding directions from the substitutional Zn sites. In addition, substitutional Zn sites with isotropic Gaussian distributions of displacements, characterized by different root mean square (rms) values  $u_1$  were considered. Details regarding the experimental setup, the simulation of the emission yield for different lattice sites in ZnO, and the data analysis procedure have been reported previously [20,21,23].

## Results

Figure 1 panels (a-d) show the experimental emission yields of the sample with the highest dose of  $^{67}\text{Cu}$  (sample 4) in the as-implanted state. The best fits of theoretical patterns to the experimental yields are shown in panels (e-h) and correspond to 55(4)% of  $^{67}\text{Cu}$  on substitutional Zn sites with isotropic Gaussian rms displacements of 0.014-0.017 nm (0.14-0.17 Å) perpendicular to the four investigated axial directions [0001], [1102], [1101], and [2113]. The remaining 45% of  $^{67}\text{Cu}$  atoms, the so-called random fraction, do not cause any anisotropy in the emission channeling patterns and are hence attributed to random sites, which are sites of very low crystal symmetry or in heavily disordered surroundings. The rms displacement of the Cu atoms from the substitutional Zn sites is somewhat larger than but still comparable to the room temperature thermal vibration amplitude of Zn atoms,  $u_1(\text{Zn}) = 0.008$  nm. The experimental results and

best fits following vacuum annealing at 700°C of the same sample are shown in Fig. 2. Besides a considerable decrease in the fraction of  $^{67}\text{Cu}$  on Zn sites and an increase of the random fraction, which is illustrated by the pronounced overall decrease in anisotropy of all four patterns, there is also a qualitative change in the nature of the lattice site, which is responsible for changing the relative intensity of axial and planar channeling effects. The best fits of the rms displacements perpendicular to the [0001],  $[\perp 102]$ ,  $[\perp 1101]$  and  $[\perp 2113]$  directions were now obtained for  $u_1(^{67}\text{Cu}) = 0.030$  nm, 0.022 nm, 0.030 nm, and 0.055 nm, which is a significant increase compared to the as-implanted state. It should be pointed out that the increase in rms displacement can be caused by various scenarios. For instance, whether the probe atoms represent an ensemble with varying small displacements from Zn sites, or all of them exhibit the same fixed displacement, or a mixture of both, is very difficult to distinguish by channeling techniques. The fact that the fitted rms displacement value from the  $[\perp 2113]$  direction is considerably larger than the others suggests that the displacements of the Cu atoms are probably not isotropic in space but occur along well-defined crystal directions. We therefore tried to fit the patterns also with fixed displacements from the ideal Zn positions towards the bonding and anti-bonding directions, both within and basal to the  $c$ -axis, however, the quality of the fits was in most cases worse than for the isotropic Gaussian displacement model. A preferential direction of the displacement could therefore not be pinpointed. However, due to limitations in computing time we did not try fixed displacements other than in bonding or anti-bonding directions, which are all located within  $(11\bar{2}0)$  or equivalent planes, and we cannot exclude that the Cu atoms are displaced along other crystal directions, e.g. within the  $(01\bar{1}0)$  or equivalent planes. In addition to near-substitutional and random sites, we also tried to include, e.g., various interstitial sites in the fits, but this did not significantly improve the quality of fit, and it was thus not possible to assign any other well-defined lattice sites to Cu.



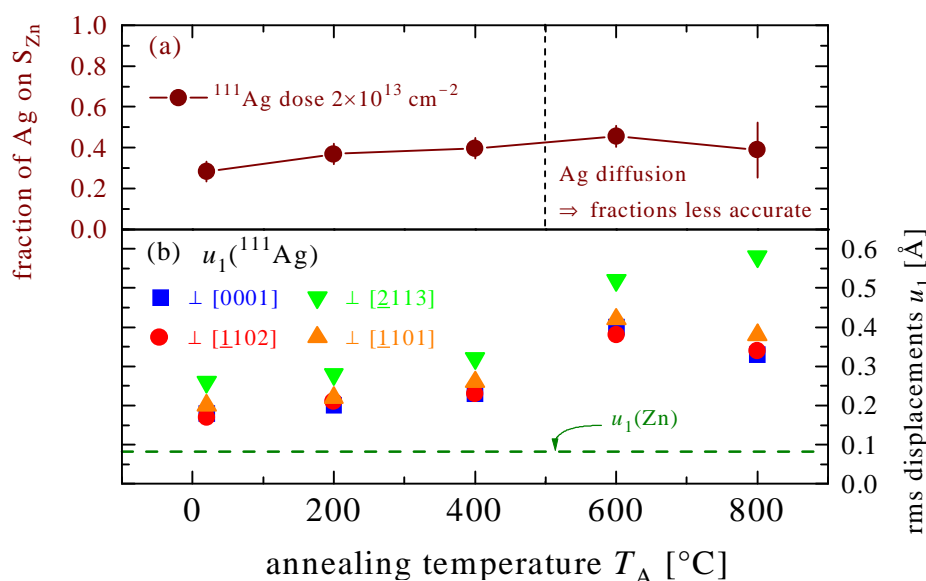
**Fig. 3:** (a) Fractions of Cu atoms on substitutional Zn sites for samples 1-4, and their room temperature rms displacements  $u_1(^{67}\text{Cu})$  perpendicular to the indicated crystal directions following 10-min annealing steps (b) for samples 1 and 2, and (c) for samples 3 and 4. The rms displacement of Zn atoms  $u_1(\text{Zn})$  due to thermal vibration at room temperature is indicated by the horizontal lines.

Figure 3 compares the fitted fractions of  $^{67}\text{Cu}$  atoms at or near substitutional Zn sites and their rms displacements for all four Cu-implanted samples. The results for sample 2, which was implanted with  $2.3 \times 10^{13} \text{ cm}^{-2}$ , have been published previously [20]. As can be seen, in all cases large fractions of Cu atoms occupy nearly ideal Zn sites in the as-implanted state, with the fraction being highest for the sample implanted with the lowest dose (sample 1) and lowest for the sample implanted with the highest dose (sample 4). The incorporation of Cu into substitutional Zn sites thus appears to be anti-correlated with the implanted dose. Annealing up to 300°C has practically no influence on the lattice location of Cu, while for annealing at 400°C the Cu rms displacements start to increase in the higher-dose implanted samples 2 and 4, but stay close to the value for ideal Zn sites in sample 1. Following annealing at 600°C, the rms displacements increase slightly in the sample 1 with lowest dose, and significantly in the other cases, with the apparent rms displacement perpendicular to the  $[\perp 2113]$  direction being considerably larger than the others. Finally, annealing at 700°C and above also caused significant decreases in the fraction of Cu on or near Zn sites in all cases. However, the fractions for annealing temperatures above 600°C are marked as less accurate since the possible diffusion of Cu may have changed the depth profile. While possible diffusion is expected to influence the fitted fractions, as was discussed previously [20,21], it does not have a pronounced influence on the identification of the rms displacements. In the case of sample 2

partial out-diffusion of several percent of the Cu activity was observed during annealing at 800°C, and therefore samples 1 and 3 were subsequently only annealed at 700°C maximum in order to avoid contamination of the emission channeling setup.

Sample 3 was only annealed once in a quartz crucible at 800°C under O<sub>2</sub> atmosphere, which resulted in a ~50% loss of implanted <sup>67</sup>Cu radioactivity. This loss is not included in the corresponding fraction shown in Fig. 3, which is normalized to the amount of <sup>67</sup>Cu remaining in the sample. Hence around 40% of the remaining Cu atoms (corresponding to around 20% of the implanted dose) still occupied sites with relatively small displacements from ideal Zn positions following the 800°C anneal.

The results from the <sup>111</sup>Ag implanted sample [21] are shown in Fig. 4, and are similar to the case of Cu. The main difference is that Ag was characterized by a much larger random fraction than Cu and only around 30-45% of Ag atoms were incorporated at or near substitutional Zn sites. In addition, the rms displacements of Ag from the ideal substitutional Zn positions were in all cases larger than those of Cu. Also in the case of Ag isotropic displacements resulted in the best possible fit. However, here we found that a fixed displacement of 0.03-0.05 nm from S<sub>Zn</sub> to the bond-center positions basal to the c-axis yielded a quality of fit that came close but still was somewhat worse than the chi square due to isotropic Gaussian rms displacements. Similar to Cu, the last annealing step at 800°C was also accompanied by a loss of 30% of activity from the sample.



**Fig. 4:** (a) Fraction of Ag atoms on substitutional Zn sites and (b) their room temperature rms displacements  $u_1(^{111}\text{Ag})$  perpendicular to the indicated crystal directions following 10-min annealing steps.

## Discussion

Directly following implantation large fractions of both Cu and Ag are found on almost ideal Zn positions, and the changes to sites showing larger rms displacements occur only upon annealing. The fact that we observed partial outdiffusion of Cu roughly confirms the diffusion coefficient  $D=2 \times 10^7 \exp(-4.8 \text{ eV}/kT) \text{ cm}^2/\text{s}$  of Cu in ZnO reported in the literature [8], from which one calculates a diffusion width around 60 Å following 10 min annealing at 800°C, by order of magnitude comparable to the mean implantation depth of 259(116) Å. Based on the observation that the diffusion coefficients of Cu and the self-diffusion coefficient of Zn are very similar, it was suggested that Cu diffuses mainly substitutionally in ZnO [8]. In any case it is very likely that annealing at lower temperatures already causes Cu and Ag to start diffusing and thus interacting with additional defects present in the sample. These are most likely defects created during implantation, which is suggested by the observation that following implantation at a very low dose obviously Cu does hardly change to sites with larger displacements. However, the annealing conditions also can play a certain role, since annealing under oxygen lean or oxygen rich conditions can change the point defect equilibrium in the near-surface Cu implanted region of the samples. Another possibility to interpret the large displacements is that they are due to the formation of Cu-Cu pairs or clusters of several Cu atoms. Since diffusion of Cu would also be required for the formation and the complexes are more likely to be formed at high Cu concentrations, this would also qualitatively explain that the large rms displacements only occur upon annealing and the dose dependence of the effect. The existence of Cu<sub>Zn</sub>-Cu<sub>Zn</sub> pairs has also previously been suggested by Müller and Helbig [8]. The high random fraction in the case of Ag shows that it is more difficult to incorporate this element in substitutional Zn sites than Cu. Possibly Ag atoms occupy

to a large extent interstitial sites of low symmetry or tend to form small precipitates. We would like to remark that there also exist transition metals that show a different behaviour in ZnO. For instance, Fe was to nearly 100% incorporated on ideal substitutional Zn sites following vacuum annealing at 800°C and did not show similar large displacements as Cu or Ag even after annealing at 1050°C [25].

The possibility that the observed displacements of Cu and Ag occur along well-defined crystal directions will be investigated further by comparing the existing experimental data to simulations for additional lattice sites, for instance positions which are displaced from ideal Zn sites within the (0110) or equivalent planes. Further experiments with different implanted doses (especially higher doses) and different annealing procedures will possibly also shed more light on whether Cu and Ag simply interact with implantation defects or form transition metal clusters.

### Conclusions

Implanted Cu and Ag show a similar behaviour in ZnO, both are capable of occupying two types of lattice sites, almost ideal Zn sites and sites that show displacements around 0.02-0.05 nm from the ideal Zn positions. The fact that the displaced substitutional sites are only found upon annealing, together with the dose dependence of the site change effect in the case of Cu, points out that both Cu and Ag change their lattice configuration when interacting with defects in ZnO. The observed incorporation of Cu and Ag on non-ideal lattice sites can possibly explain that these impurities do not exhibit simple acceptor behaviour in ZnO, existing mainly bound in complexes with other defects or as pairs or even clusters of several atoms.

### Acknowledgments

This work was funded by the Foundation for Science and Technology/Portugal (FCT), project PDCT-FP-FNU-50145-2003, and by the European Commission through the HPRI program (Large Scale Facility contract Nr HPRI-CT-1999-00018). UW and ER acknowledge their fellowships from FCT.

### References

- [1] S.J. Pearton, D.P. Norton, K. Ip, Y.W. Heo, and T. Steiner, *J. Vac. Sci. Technol. B* 22 (2004) 932.
- [2] R. Dingle, *Phys. Rev. Lett.* 23, 579 (1969).
- [3] H.J. Schulz and M. Thiede, *Phys. Rev. B* 35, 18 (1987).
- [4] P. Dahan, V. Fleurov, P. Thurian, R. Heitz, A. Hoffmann, and I. Broser, *J. Phys.: Condens. Matter* 10, 2007 (1998).
- [5] N.Y. Garces, L. Wang, L. Bai, N.C. Giles, L.E. Halliburton, and G. Cantwell, *Appl. Phys. Lett.* 81, 622 (2002).
- [6] G. Bogner and E. Mollwo, *J. Phys. Chem. Solids*, 6, 136 (1957).
- [7] G. Bogner, *J. Phys. Chem. Solids*, 19, 235 (1961).
- [8] G. Müller and R. Helbig, *J. Phys. Chem. Solids*, 32 (1971) 1971.
- [9] Y. Kanai, *Jpn. J. Appl. Phys. I* 30 (1991) 703.
- [10] Y. Kanai, *Jpn. J. Appl. Phys. I* 30 (1991) 2021.
- [11] J. Fan, R. Freer, *J. Appl. Phys.* 77 (1995) 4795.
- [12] P.J. Dean, D.J. Robbins, S.G. Bishop, J.A. Savage, and P. Porteous, *J. Phys. C: Sol. State Phys.* 14, 2847 (1981).
- [13] A.F. Kohan, G. Ceder, D. Morgan, and C.G. Van De Walle, *Phys. Rev. B* 61, 15019 (2000).
- [14] D.C. Reynolds, D.C. Look, and B. Jogai, *J. Appl. Phys.* 89, 6189 (2001).
- [15] B. Lin, Z. Fu, and Y. Jia, *Appl. Phys. Lett.* 79, 943 (2001).
- [16] K. Vanheusden, W.L. Warren, C.H. Seager, D.R. Tallant, J.A. Voigt, and B.E. Gnade, *J. Appl. Phys.* 79, 7983 (1996).
- [17] X.L. Wu, G.G. Siu, C.L. Fu, and H.C. Ong, *Appl. Phys. Lett.* 78, 2285 (2001).
- [18] S.B. Zhang, S.H. Wei, and A. Zunger, *Phys. Rev. B* 63, 75205 (2001).
- [19] T. Agne et al, to be published.
- [20] U. Wahl, E. Rita, J.G. Correia, E. Alves, J.C. Soares, and the ISOLDE collaboration, *Phys. Rev. B* 69 (2004) 012102.
- [21] E. Rita, U. Wahl, A.M.L. Lopes, J.P. Araújo, J.G. Correia, E. Alves, J.C. Soares, and the ISOLDE collaboration, *Physica B* 69 (2003) 240.
- [22] H. Hofsäss and G. Lindner, *Phys. Rep.* 210 (1991) 121.
- [23] U. Wahl, J.G. Correia, A. Czermak, S.G. Jahn, P. Jaçocha, J.G. Marques, A. Rudge, F. Schopper, J.C. Soares, A. Vantomme, P. Weilhammer, and the ISOLDE collaboration, *Nucl. Instr. Meth. in Physics Research A* 524 (2004) 245.
- [24] U. Wahl, A. Vantomme, G. Langouche, J.P. Araújo, L. Peralta, J.G. Correia, and the ISOLDE collaboration, *J. Appl. Phys.* 88 (2000) 1319.
- [25] E. Rita, U. Wahl, J.G. Correia, E. Alves, J.C. Soares, and the ISOLDE collaboration, *Appl. Phys. Lett.* 85 (2004) 4899.